Circulation in the Gulf of Trieste: Measurements and model results

B. Bogunović(*) and V. Malačič

Marine Biology Station, National Institute of Biology - Piran, Slovenia

Summary. — The study presents seasonal variability of currents in the southern part of the Gulf of Trieste. A time series analysis of currents and wind stress for the period 2003-2006, which were measured by the coastal oceanographic buoy, was conducted. A comparison between these data and results obtained from a numerical model of circulation in the Gulf was performed to validate model results. Three different approaches were applied to the wind data to determine the wind stress. Similarities were found between Kondo and Smith approaches while the method of Vera shows differences which were particularly noticeable for lower ($= 1$ m/s) and higher wind speeds ($= 15$ m/s). Mean currents in the surface layer are generally outflow currents from the Gulf due to wind forcing (bora). However in all other depth layers inflow currents are dominant. With the principal component analysis (PCA) major and minor axes were determined for all seasons. The major axis of maximum variance in years between 2003 and 2006 is prevailing in NE-SW direction, which is parallel to the coastline. Comparison of observation and model results is showing that currents are similar (in direction) for the surface and bottom layers but are significantly different for the middle layer (5–13 m). At a depth between 14–21 m velocities are comparable in direction as well as in magnitude even though model values are higher. Higher values of modelled currents at the surface and near the bottom are explained by higher values of wind stress that were used in the model as driving input with respect to the stress calculated from the measured winds. Larger values of modelled currents near the bottom are related to the larger inflow that needs to compensate for the larger modelled outflow at the surface. However, inspection of the vertical structure of temperature, salinity and density shows that the model is reproducing a weaker density gradient which enables the penetration of the outflow surface currents to larger depths.

PACS `92.10.A-` – Circulation and currents.
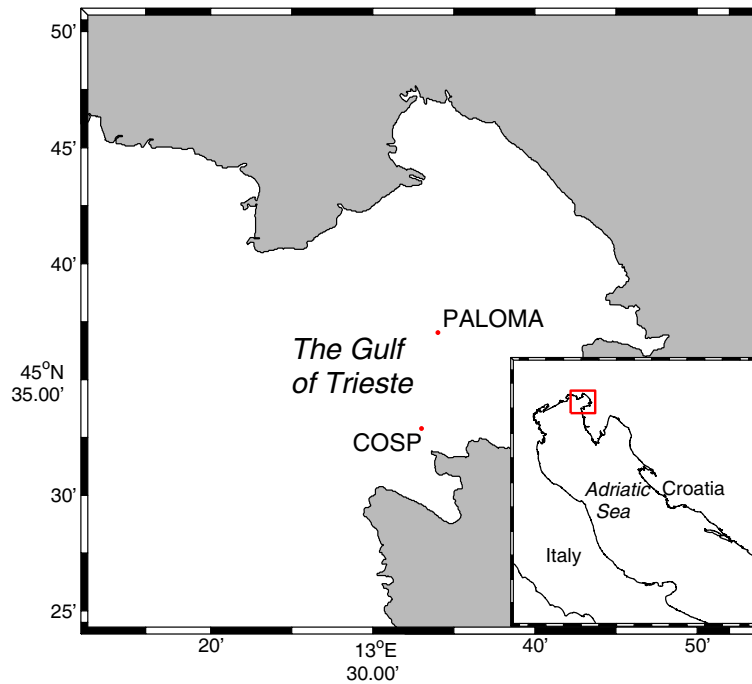
(*) E-mail: `bogunovic@mbss.org`

Fig. 1. – Study area—Gulf of Trieste (North Adriatic), and position of the coastal buoy COSP and PALOMA.

1. – Introduction

The region of the Gulf of Trieste (Gulf) is a semi-enclosed basin and is situated in the north Adriatic Sea (fig. 1). The Gulf has received considerable oceanographic attention in the last two decades due to its dynamic ocean environment and importance in activities such as tourism and maritime transport that are directly dependent on the sea conditions.

Even though the Gulf is limited in size ($20 \, \text{km} \times 20 \, \text{km}$) and particularly in depth ($24 \, \text{m}$) it plays a role in the circulation of the Northern Adriatic Sea. In general, circulation of the Gulf is driven by interplay of different forcings: wind stress (particularly bora), buoyancy fluxes and general circulation of the Adriatic Sea [1], together with tides and seiches.

In winter, the northern Adriatic is subject to strong ENE winds, called bora, blowing south-westward from the mountainous eastern coast. Bora winds have strong horizontal shear because of localized blocking by east-coast topography [2]. Some observations that were conducted in the southern entrance of the Gulf showed that after a wind episode during warming seasons the surface layer is separated from the layer below by a sharp pycnocline [3]. The authors of ref. [4] found close correlation between the surface current in the Gulf and wind velocity produced by Bora events in winter situation. In the surface layer there is an outflow current from the Gulf.

In the late 90s current meter measurements were conducted with the acoustic Doppler current profiler (ADCP) in the southern edge of the Gulf during spring period [5]. The current velocities showed a similar pattern through all water columns—inflow currents.

It was shown that the surface wind-driven Ekman layer and the bottom Ekman layer overlap and thus the entire flow is affected simultaneously by the surface wind, bottom friction and the Coriolis force.

Short-time series analysis of currents during winter (November 2002 to February 2003) showed a typical situation: an outflow from the Gulf at the surface and an inflow at depth along the southern (Slovenian) coastline [6]. Moreover, results obtained from the ACOAST-2 model during winter period are also showing an outflow in the surface layer and an inflow over the majority of water column below the surface wind-driven layer [7].

However, the climatology for the entire year is still experimentally unclear and there are some aspects of the water circulation in the Gulf of Trieste that deserve attention.

The goal of this study is to analyse current-meter observations and to deduce from them the seasonal character of currents that flow along the southern coastline of the Gulf.

The second goal is to determine whether the results from the model of climatic circulation are consistent with measurements. Differences will also be explored in light of different wind stress, which is applied in climate studies and is also calculated from wind measurements during the current-meter observations.

This is particularly true for the wind stress which in most cases determines the vertical structure of currents in a confined basin and consequently influences the water exchange between the Gulf and the rest of the Adriatic.

2. – Material and methods

The time series analysis of currents for the period 2003-2006, which were measured by the Acoustic Current Meter Profiler (ADCP) placed below the coastal oceanographic buoy Piran (COSP), were conducted. The buoy is situated in the southern part of the Gulf of Trieste (45°32.90′ N, 13°33.00′ E), 1.23 nautical mile from the shore (fig. 1).

Current-meter data were retrieved by the on-board electronics of the buoy from the ADCP instrument placed at the sea-bottom, at a depth of 22 m. Data were collected in bins of a thickness of 1 m, one vertical profile of currents is composed of 20 cells (meters). For a clearer interpretation of the data, bins were vertically assembled over layers of thickness of 4 m, thus five thicker layers were composed: 1–4 m depth (first layer below the sea-surface); 5–8 m depth; 9–12 m depth; 13–16 m depth and 17–21 m depth (last layer above the sea bed).

Data of these vertically averaged currents were thereafter examined for gaps that appeared in the time series with a sampling period of 0.5 h. In case of relatively small gaps (< 4 h) data were linearly interpolated, otherwise the data were separated in groups of time series and each group was analysed. Since tidal currents do not play an important role in the water exchange to the Gulf the tidal signal was removed. Since data sampling has a period of 0.5 h the proper filter has to be applied to take half an hour values into account, therefore the tidal signal was removed by applying a low-pass filter—"pl66" [8].

Principal axes (PCA) of velocity variance were calculated for five different depth layers. We are interested in the variation of variance of currents through different seasons. Therefore, seasons in this paper were chosen as three-month periods: Spring is March-May, Summer is June-August, Autumn is September-November and Winter is defined as December-February. The PCA method in oceanography is commonly known as the empirical orthogonal function (EOF) [9]. Principal components are linear combinations of variables and subject to two constraints: the total variance must remain the same and
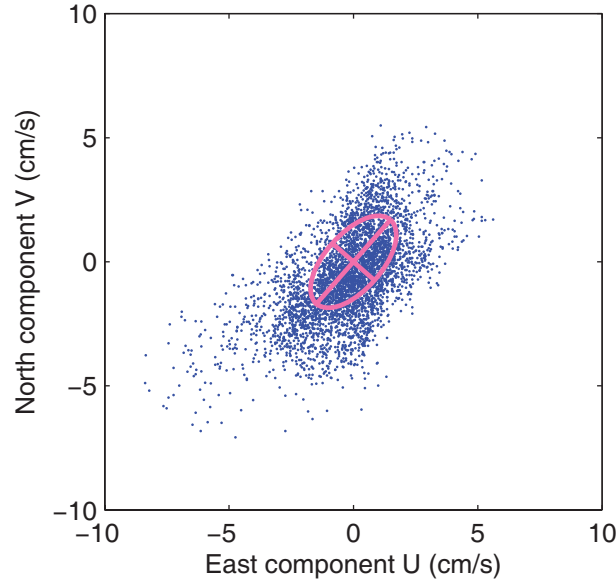
Fig. 2. – The principal axis ellipse with the scatter plot of velocities measured for 10 minutes every half hour from COSP at 10 m depth.

the components must be uncorrelated. When there are only two components, the first component has the largest possible variance along the major axis; the second component is uncorrelated with the first one and has the remaining variance along the minor axis of the variance of currents. We are looking for the principal axes, u' (east component) and v' (north component) which are the respective east and north components of the velocity fluctuations, obtained by removing their mean values $\bar{u}$ and $\bar{v}$ from each record: $u' = u - \bar{u}$, $v' = v - \bar{v}$. The amount of data "scatter" is maximum along the major axis and is minimum along the minor axis (fig. 2). The eigenvalue problem $\mathbf{C}\boldsymbol{\phi} - \lambda\mathbf{I}\boldsymbol{\phi} = 0$ for the two-dimensional scatter plot has the form

$$(1) \qquad \begin{vmatrix} C_{11} & C_{21} \\ C_{12} & C_{22} \end{vmatrix} \begin{vmatrix} \phi_1 \\ \phi_2 \end{vmatrix} = \begin{vmatrix} \lambda & 0 \\ 0 & \lambda \end{vmatrix} \begin{vmatrix} \phi_1 \\ \phi_2 \end{vmatrix},$$

where C_{ij} are the components of the covariance matrix $\mathbf{C}$ where i or $j = 1, 2$ (ϕ_1, ϕ_2) are the unknown eigenvectors associated with the two possible values of the unknown eigenvalues, λ [9].

$$(2) \qquad C_{ii} = \overline{u'^2_i} = \frac{1}{N} \sum_{n=1}^{N} [u'_i(t_n)]^2,$$

$$(3) \qquad C_{ij} = \overline{u'_i u'_j} = \frac{1}{N} \sum_{n=1}^{N} [u'_i u'_j(t_n)].$$

The covariance matrix equation (4) has a solution only when the determinant is set to

zero:

$$(4) \qquad \det |C - \lambda \mathrm{I}| = \det \begin{vmatrix} \overline{u'^2} - \lambda & \overline{u'v'} \\ \overline{v'u'} & \overline{v'^2} - \lambda \end{vmatrix} = 0.$$

The eigenvalues follow as solutions of the quadratic equation:

$$(5) \qquad \lambda^2 - \left[\overline{u'^2} + \overline{v'^2}\right]\lambda + \overline{u'^2 v'^2} - \left(\overline{u'v'}^2\right) = 0,$$

as

$$(6) \qquad \lambda_{1,2} = \frac{\left[\overline{u'^2} - \overline{v'^2}\right]}{2} \pm \frac{\sqrt{\left[\overline{u'^2} - \overline{v'^2}\right] + 4(\overline{u'v'}^2)}}{2} \ .$$

The orientations of the two axes (eigenvectors) differ by 90° and the principal angle θ_p of the major one is found through the relation

$$(7) \qquad \theta_p = \frac{1}{2}\tan^{-1}\left[\frac{2\overline{u'v'}}{\overline{u'^2} - \overline{v'^2}}\right].$$

It is expected that the major axis would be oriented along the coastline due to the proximity of the coast. In most cases the major principal axis is used to define the "long-shore" direction of velocity fluctuations while the minor axis defines the "cross-shore" of the flow [9]. Since in the Gulf coastal winds, particularly Bora, are prevailing along the axis of the Gulf they directly influence the orientation of the major axis.

Average velocities each year and each season in the year were also calculated. Inter-annual variations of seasonal currents for the period 2003-2006 were followed. The analysis of the wind data measured on the coastal buoy was also conducted to find correlations between the wind stress and currents.

The wind data were retrieved by the on-board electronics from the anemometer of the coastal buoy which is placed $5\,\mathrm{m}$ above the sea level. The data were collected in $0.5\,\mathrm{h}$ and the low-pass filter ("pl66") was applied to remove daily sea breeze from the wind and comparison between the wind stress from experimental and model data was conducted. Therefore, wind stress was calculated from the wind data. First we adjusted the wind data to the reference level at $10\,\mathrm{m}$ height (U_{10}) as shown in fig. 3. Thereafter, the drag coefficient (C_d) was calculated to obtain the wind stress. We tested the wind data for obtaining C_d with different recipes:

First recipes by [10] define the drag coefficient:

$$(8) \qquad C_d = \left[\frac{\ln(10/z_0)}{\kappa}\right]^{-2},$$

where $\kappa = 0.41$ Von Karman's constant; z_0 is the roughness length (in meters) calculated:

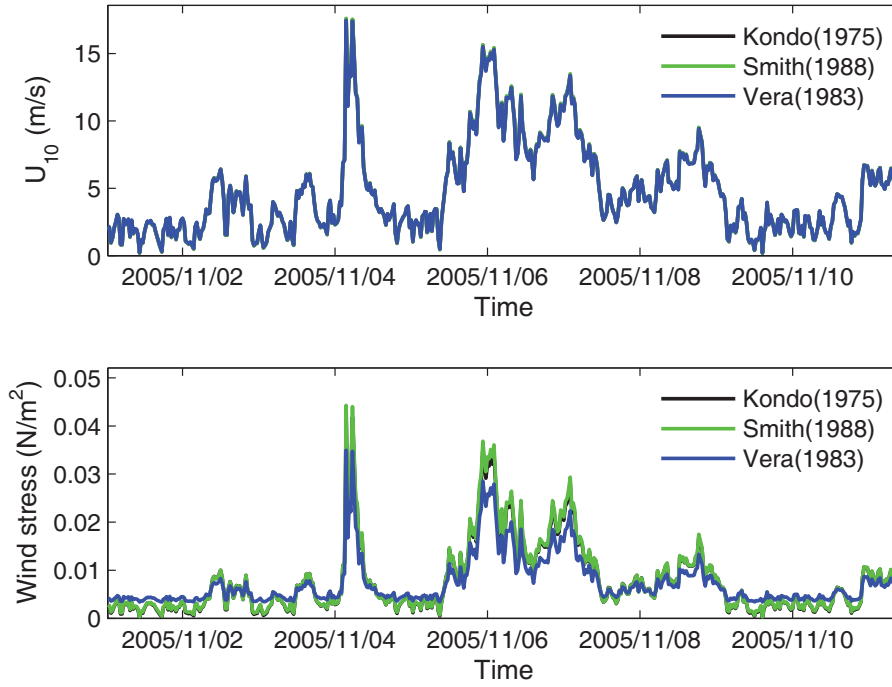$$(9) \qquad z_0 = \exp\left[\ln(10) - \kappa \left[C_{d10}\right]^{-1/2}\right],$$

Fig. 3. – (Top) Calculation of the wind velocity (U_{10}) at reference level $10\,\text{m}$—comparison between different recipes. (Bottom) Figure represents wind stress by applying different methods. It can be seen that [10] and [11] have similar values and that values from [12] are significantly different for higher wind velocity (above $15\,\text{m/s}$).

where

$$(10) \qquad\qquad C_{\text{d}10} = a_{\text{d}} + b_{\text{d}} u_{10}^{p_{\text{d}}},$$

where a_{d}, b_{d} and p_{d} are numerical constants, which vary with the range of the wind speed.

The reference wind velocity at $z = 10\,\text{m}$ height was calculated:

$$(11) \qquad\qquad u_{10} = \frac{u_z \ln(10/z_0)}{\ln(z/z_0)} .$$

Since the known value is u_z and not u_{10}. In practical application, the estimation of the drag coefficient (C_{d}) was performed by successive approximations, starting with the initial assumption that $u_{10} = u_z$. From there we obtain the approximate value of $C_{\text{d}10}$ from eq. (10).

By inserting the value $C_{\text{d}10}$ into eq. (9) we obtain the approximate value of u_{10} with the use of eq. (11). In this study, three iterations were found to be sufficient. From there the drag coefficient was calculated using eq. (8).

Second, recipes by Vera and published by [12] are defining the drag coefficient

$$(12) \qquad C_{\mathrm{d}10} = \left(\frac{u^*}{u_{10}}\right)^2,$$

where the square of the friction velocity u^* is defined as

$$(13) \qquad u^{*2} = 10^{-3}(2.717u_{10} + 0.142u_{10}^2 + 0.0764u_{10}^3)$$

and where u_{10} represents the wind speed at $z = 10\,\mathrm{m}$, calculated from eq. (11).

Third, recipes by [11] are defining the drag coefficient at the $z = 10\,\mathrm{m}$ same as [10]

$$(14) \qquad C_{\mathrm{d}10} = \left(\frac{\kappa}{\ln(10/z_0)}\right)^2,$$

however z_0 is calculated with different terms:

$$(15) \qquad z_0 = \frac{0.018u_*^2}{g} + \frac{0.11\nu}{u_*},$$

where $g = 9.81\,\mathrm{m/s^2}$ is the gravitational acceleration; $\nu = 14 \times 10^{-6}\,\mathrm{m^2/s}$ is the kinematic viscosity of air and u_* is the frictional velocity defined as

$$(16) \qquad u_* = \tau/\rho_{\mathrm{a}}.$$

Wind stress was defined by the equation

$$(17) \qquad \tau = C_{\mathrm{d}10}\rho_{\mathrm{a}}u_{10}^2,$$

where ρ_{a} is the density of air calculated from temperature and humidity.

Before we could calculate the wind stress, the drag coefficient, which enters in the calculation of the stress from the wind velocity, was tested and calculated with three different methods on wind time series. The comparison of C_{d} values is presented in fig. 4. [10] and [11] approaches give very similar C_{d} values. They however, differ up to 50% for winds speeds lower than $1\,\mathrm{m/s}$.

Some unusual $C_{\mathrm{d}10}$ values were obtained by [12] approach and in comparison with the other two recipes they are almost ten times higher (fig. 4). Drag coefficient values from [12] are showing extremely high values for low wind speeds ($\leq 2\,\mathrm{m/s}$) (fig. 4). It can be noted from fig. 3 that wind stress from [12] is different for high- and low-wind speeds comparing with the two other methods. Therefore, for the calculation of the wind stress we used the approach of [10].

The input data for wind stress that were used for the numerical model were obtained from the winds of the 1982-1993 ECMWF surface re-analysis [13], according to the expressions of [14]. The wind values were enlarged for a factor of 1.5, following [15] who studied surface waves in the northern Adriatic. This correction was applied to climatic circulation studies by [16,17], and [7]. Wind stress was averaged monthly over perpetual years.

For the purpose of this study currents obtained from the model ACOAST-2 with horizontal resolution of $500\,\mathrm{m}$ were taken as reference climatic currents [7]. Currents were
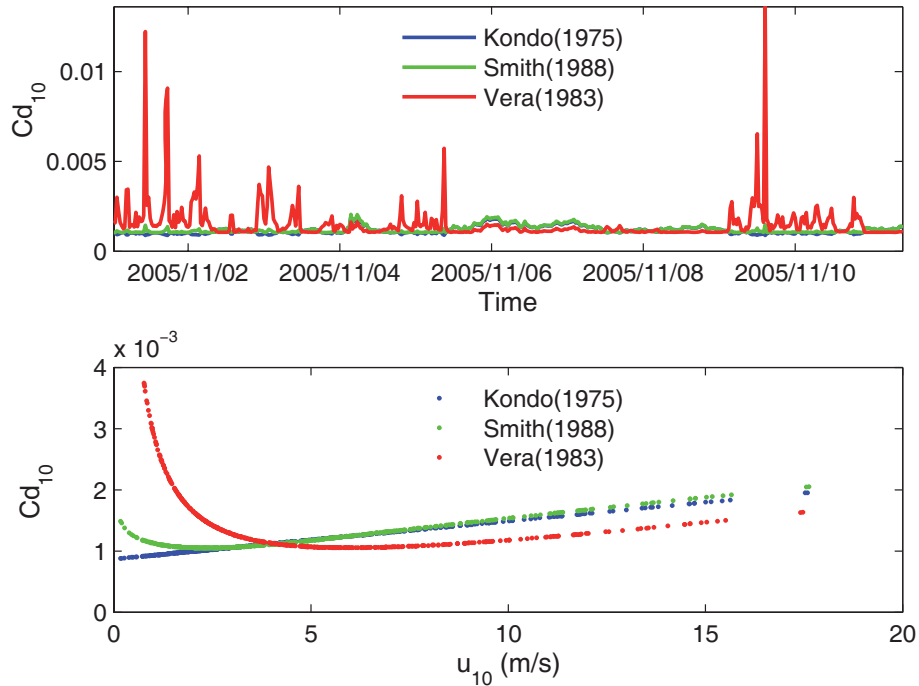
Fig. 4. – (Top) Comparison of drag coefficient calculated by different methods. (Bottom) figure—drag coefficient of the sea surface for a reference height of 10 m *vs.* the wind speed.

extracted from the model cells at different depths, the locations of which correspond to the position of the coastal buoy. The model is nested in a coarser model of the climatic circulation of the northern Adriatic [17].

To observe differences between the wind stresses used in the climatic circulation model of the Gulf and the ones obtained from measurements, we performed monthly averaging of experimental data. Model results are validated by comparison between the time series analysis of measured currents and the results obtained from a numerical model of circulation.

ACOAST-2 model is the Princeton Ocean Model (POM) which is using sigma stretched coordinate along the vertical $\sigma = z/D$, where D is the water depth. Eleven sigma values range from 0 (surface) to -1 (bottom), they are unevenly spaced to resolve rapid vertical changes in the surface and bottom layers.

The ACOAST-2 model (0.5 km of horizontal resolution) is one-way nested in the Northern Adriatic Shelf Model (NASM, horizontal resolution of 1.5 km), created by [17]. From the objective analysis of the ATOS (Adriatic Temperature, Oxygen and Salinity) database [18] seasonal temperature and salinity was obtained for the initialization of NASM. The model of the Gulf is initialized with the interpolation on a model grid of 10-day averages of temperatures and salinities for the first ten days of climatic January, which are the model results of the coarser NASM.

In the ACOAST-2 model the diagnosed values of monthly averages of heat fluxes from numerical simulations of NASM were applied to the sea-surface for the heat flux and precipitation-evaporation [17], which were interpolated to a finer grid of 0.5 km. All

forcing fields at the surface, including wind stress, varied linearly with time between monthly averages. Since linear variations between monthly values do not conserve the time integral of quantities, a correction procedure was applied to monthly averages [19], and monthly pseudovalues were utilized instead.

Rivers in the ACOAST-2 were considered in a different manner than that in [17], where river flows were considered through lower values of salinity in surface cells around river discharge locations. In ACOAST-2 the model topography was adapted to mimic the river estuary along the model grid-line inside the land-domain, where the width of estuaries equals the horizontal dimension of the grid-cells (0.5 km). It is sufficient to impose about ten model cells "upstream" from the river mouth along the estuary. If the topography data of the estuary are not known, it is assumed that the depths of estuaries decrease linearly from the depth at the mouth towards a depth of 2 m at the upstream end. In this work, monthly values of river flow-rates were imposed on the uppermost stream cells in all sigma-layers through the depth-averaged velocities in the downstream direction [20]. The salinity in most upstream cells is zero. The sea-surface elevation was extrapolated from the elevation in cells that neighbour the river mouths. This holds also for temperature, since climatic monthly temperatures of rivers in estuaries were not known.

Simulations with the nested model of the Gulf clearly showed a false narrow strip of low salinity along its southern coastline, therefore a better representation of river fluxes than that in [21] became a necessity. New river data sources used in the ACOAST-2 model are more reliable as far as the peninsula of Istria is concerned. However, the model domain covers a much larger area than the Gulf of Trieste, and river inflows from all sources along the northern Italian coastline between the Soča (Isonzo) river outlet and the end of the coastline in the model domain (Tagliamento) have been considered as described in the NASM.

The model was run for three perpetual years and the results from the third year, which differ insignificantly from the run of the second year, have been taken as relevant for this study.

Results from model were interpolated from the sigma layers to the z layers of fixed depths which correspond to the depths of cells of ADCP data of COSP so that model results are comparable with the experimental data. Model results of currents were also averaged in seasons of all four years 2003-2006. Therefore the analysed data were grouped and sorted in 36 decades for comparison with model results. The averaging of buoy current over one perpetual climatic year applied in the model includes 36 decades (each decade is 10 days long).

PCA analysis was applied to 55 vertical CTD (conductivity-temperature-depth) casts near COSP in the period 2003-2006 to evaluate the variation of the main variance through a year and compare this with the main variance of PCA analysis of the model values of temperature, salinity and density. Since CTD measurements were performed at least twice a month, therefore it was necessary to sort and group the data in the same manner as the model data, one in 36 decades. Temperature and salinity data were vertically averaged every 0.5 m. The PCA analysis was performed on each parameter separately: on temperature, salinity and also on the resulting density. The time evolutions of the first three PCA modes through a perpetual year determine how the vertical distribution of quantities is changing through a year. This was compared to the evolution of three dominant PCA modes of modelled data. The main emphasis was on the spring to autumn period when stratification plays an important role. Unfortunately, the majority of weekly CTD casts were taken in year 2003 during the ADRICOSM project, while in

the period 2004-2006 casts were taken once or twice per month. Since the year 2003 was exceptionally dry and hot [22] we expect that vertical profiles of temperature and salinity will be biased towards higher temperatures and salinities during the stratified period.

In the final part of the analysis the input data for wind stress in the model were compared with the wind stress calculated from winds measured at COSP and PALOMA. This comparison reveals if differences in wind forcing are related to the differences between modelled and measured currents. Seasonal variations of the wind forcing that lead to different currents were also observed.

3. – Results and discussion

3˙1. *Results obtained from the principal component analysis of the ADCP currents*. – *Winter situation*: For the first layer (1–4 m depth) the major axis of maximum variance in years 2003-2006 is parallel to the coastline (fig. 5a). Averaged velocity for this surface layer for all years (2003-2006) is showing an outflow from the Gulf. This is due to Bora wind (NE) which could be considered as the main driving agent that is pushing water in the surface layer out of the Gulf. However, in the second layer (5–8 m depth) the reverse mean current is dominant (fig. 5b) into the Gulf. The major axis of maximum variance for three years (2003-2005) is similar to the one in the first layer (SW-NE), while for the year 2006 the highest variance of currents is orthogonal to the direction of the major variance in the layer above.

In depths between 9 and 13 m (third layer) the average velocity is showing an inflow with a smaller deviation from it in years 2003 and 2006, when mean currents are oriented towards the Slovenian coastline (fig. 5c). The variance of currents has a pattern similar to the previous layer, in (SW-NE) direction, with a small deviation in direction in year 2006 where the major axis is in N-S direction. In the fourth layer depths 14–17 m, the major axis for all four years is parallel to the coastline, while the average current in depth is in the same direction—there is an inflow current as shown in fig. 5d. Furthermore, in the deepest layer (18–22 m depth) the major axis of variance is showing the same direction (SW-NE) as in layers above and the average velocity is again showing an inflow current (fig. 5e).

Spring situation: in the first layer a strong outflow is present in all years (2003-2006). Even though the Bora wind is less frequent in spring than in winter, it still has a strong impact on surface layer (fig. 6a). Direction of the major axis is close to in W-E direction. However, in year 2006 the major variance of currents is in N-S direction, which is similar to the winter situation at depth 9–13 m. In the second layer (fig. 6b) below the first one, the average velocity for all years is generally showing the inflow current. Moreover, the major axis of variance is almost the same to the one in winter, with the deviation in direction SE-NW in year 2006. In the third layer (fig. 6c) the major axis is roughly parallel with the coastline and the average velocity is showing an inflow current.

The deepest two layers (figs. 6d and 6e) are also showing the major axis of variance along the coastline, while the average velocity is showing the inflow current. For years 2004 and 2005 the inflow is more directed towards Slovenian coastline, which is similar to the winter situation for depths between 9–17 m depth.

Summer situation: Principal axes of velocity variance are similar for all five layers; they are aligned with the coastline (fig. 7a-7e) or with the Gulf's axis in year 2006. However, there are some differences in the direction of the average velocity between layers. The mean outflow current is present in the surface layer (first one) in years 2005 and 2006, while in the other two years (2003-2004) there is the mean inflow current
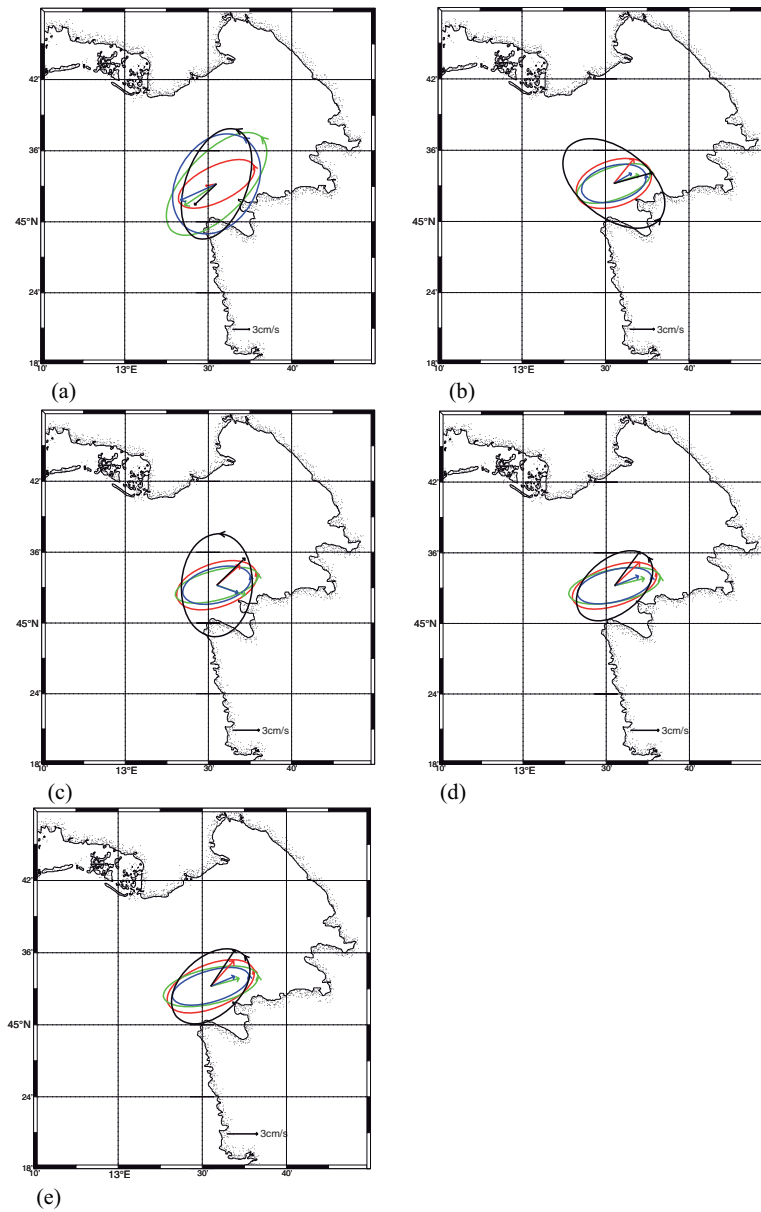
Fig. 5. – (a) Winter situation. Mean currents (arrows) and principal ellipses for observed velocities; 2003 (red), 2004 (green), 2005 (blue), 2006 (black). First layer (1–4 m depths), (b) second layer (5–8 m depths), (c) third layer (9–13 m depths), (d) fourth layer (14–17 m depths), (e) fifth layer (18–21 m depths).
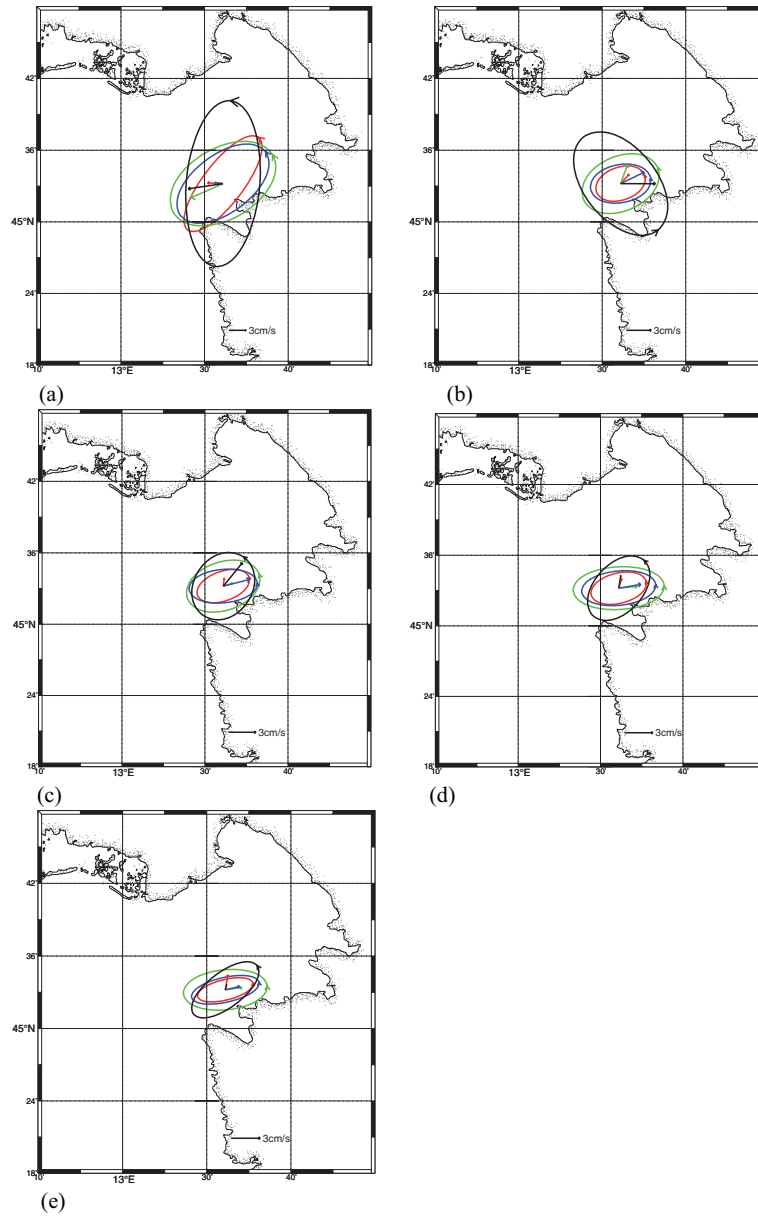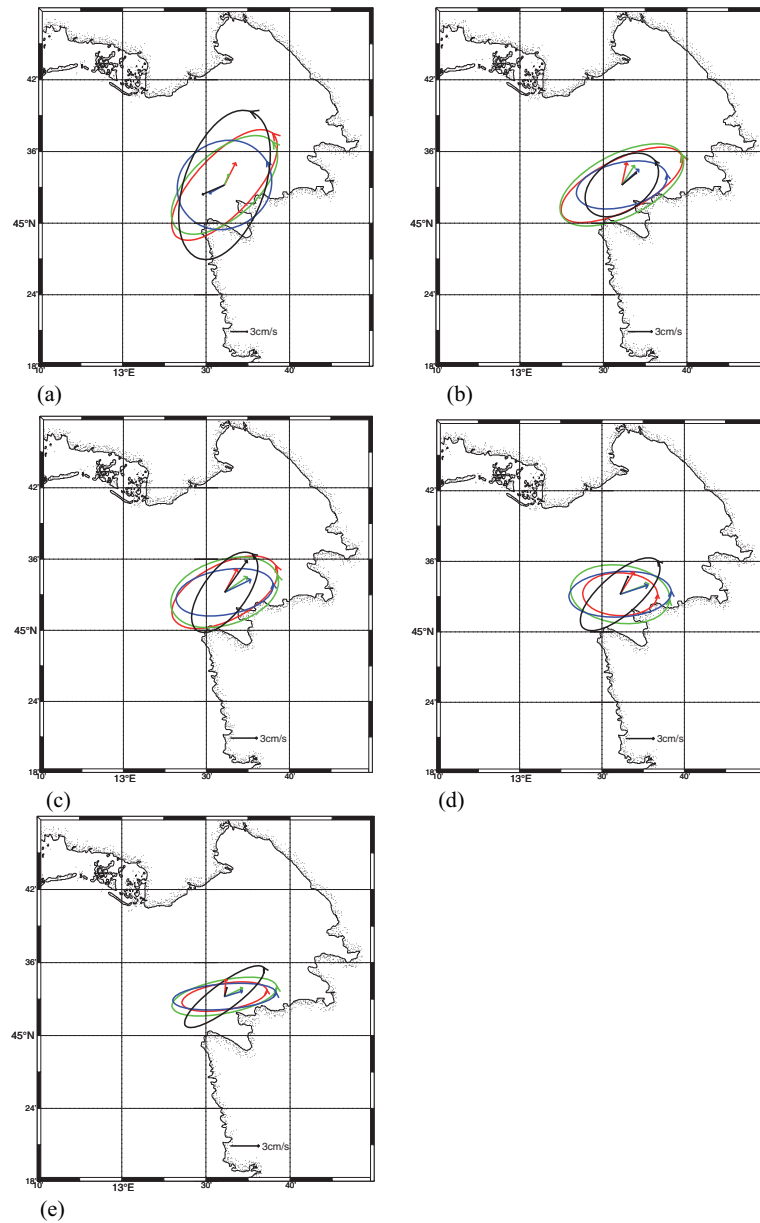
Fig. 6. – (a) Spring situation. Mean currents (arrows) and principal ellipses for observed velocities; 2003 (red), 2004 (green), 2005 (blue), 2006 (black). First layer (1–4 m depths), (b) second layer (5–8 m depths), (c) third layer (9–13 m depths), (d) fourth layer (14–17 m depths), (e) fifth layer (18–21 m depths).

Fig. 7. – (a) Summer situation. Mean currents (arrows) and principal ellipses for observed velocities; 2003 (red), 2004 (green), 2005 (blue), 2006 (black). First layer (1–4 m depths), (b) second layer (5–8 m depths), (c) third layer (9–13 m depths), (d) fourth layer (14–17 m depths), (e) fifth layer (18–21 m depths).

(fig. 7a). In the other four layers there is the mean current, which is decreasing with depth from mid depths (9–13 m) to the bottom.

Autumn situation: In contrast with the summer situation the mean outflow is present in the surface layer for years 2003-2004 (fig. 8a). In years 2005-2006 there is a strong inflow current which is again in contrast to the situation in the summer period. The axis of major variance in all layers (1–22 m depth) is mostly aligned with the coastline (SW-NE) (fig. 8b-8e).

3'2. *Comparison of observations of currents with the model results*. – The second part of results is concentrated on the comparison between the currents measured by COSP and numerical model results. Decadal currents are compared within a perpetual year with 36 decades.

In the first surface layer (1–4 m depth) model results are similar to the ADCP measurements: there is generally an outflow current (fig. 9a). This generally agrees with the mean current that was explained previously. However, results from the model are showing a stronger outflow in the summer period (August-September) which is a few times larger than measurements show. This significant difference can be due to wind stress, used as the input in numerical model that is larger than the stress acting at the sea surface (fig. 10). We also have to consider inter-annual variations of seasonal currents (fig. 5a-8a) at the sea surface in the second half of the year, where the change from the input flow in one year to the outflow in another gives for the average in 2003-2006 values closer to zero.

In the second layer (5–8 m) results between the experimental and model data are significantly different (fig. 9b). Results from the model are showing a strong outflow in SE direction, which is opposite to the measured currents. Generally, the model shows velocities similar to the ones in the surface layer, with lower magnitudes. Measurements at the COSP, however, are opposite to outflow currents in the surface layer over the whole year, which agrees with the seasonal mean currents for the second layer in all four seasons (fig. 5b, 6b, 7b and 8b).

In the third layer (9–12 m depth) the match between modelled inflow currents and the measured ones is much better, particularly for the first half of the year (fig. 9c). In the second half of the year results from the model are showing an outflow current from the Gulf, while measurements 2003-2006 do not reveal this in mid-depths of the water column.

In deepest layers four and five (depth 13–21 m) results from the model are quite similar to the experimental data; they show an inflow current (fig. 9d and 9e). Again, the velocity magnitudes in model results are higher than the magnitudes of measured velocities. These differences in magnitude are however significantly smaller than those in the first layer.

3'3. *PCA analyses of temperature, salinity and density*. – One of the major reasons for the discrepancy between model and measured currents in the middle (5 m–13 m) part of the water column at the position of COSP may lie in the model's capacity for solving the vertical density (temperature and salinity) stratification. In fig. 10a the vertical structure of temperature from the model simulation is shown for the stratified period (decades 10-25, April to September). It can be noticed that the temperature is showing a weak thermocline during the summer seasons (decades 15-25). However, measurements in years 2003-2006 show (fig. 10b) much stronger thermal stratification in stratified seasons, with higher temperatures for up to $7\,^{\circ}$C in the surface layers and for about $2\,^{\circ}$C near the bottom.
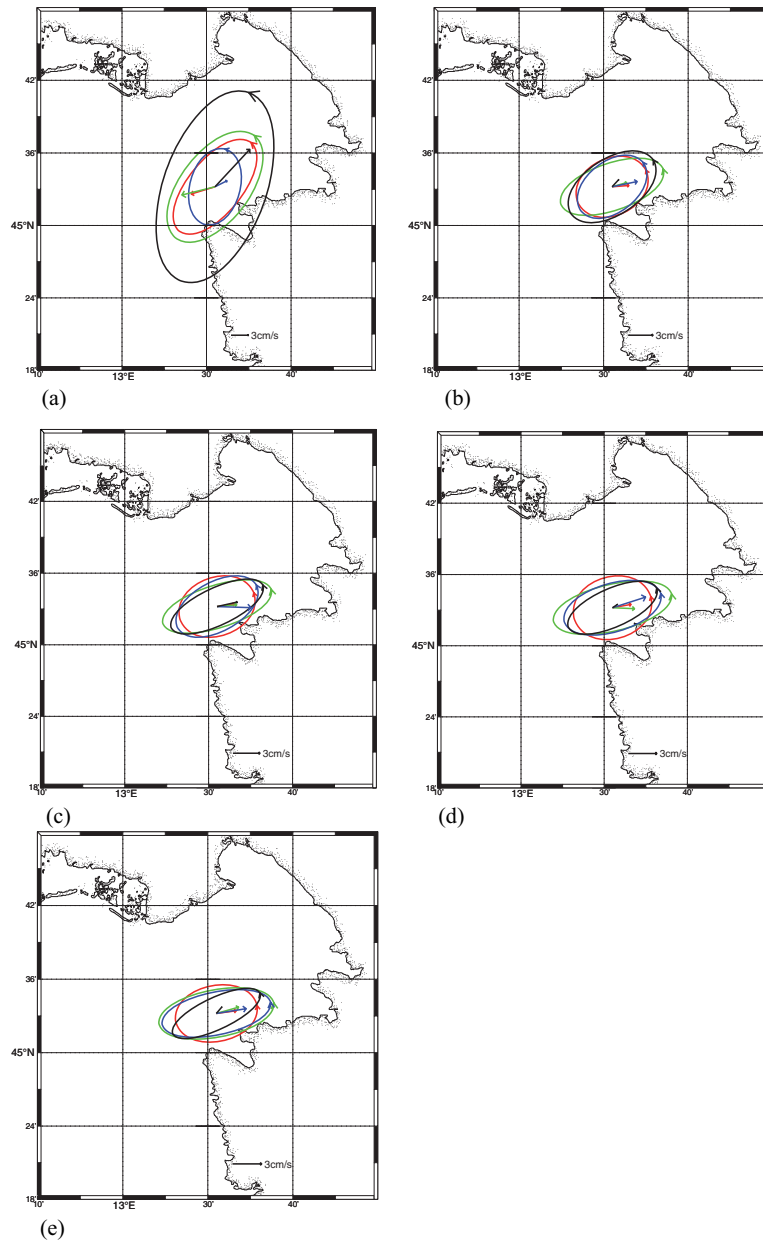
Fig. 8. – (a) Autumn situation. Mean currents (arrows) and principal ellipses for observed velocities; 2003 (red), 2004 (green), 2005 (blue), 2006 (black). First layer (1–4 m depths), (b) second layer (5–8 m depths), (c) third layer (9–13 m depths), (d) fourth layer (14–17 m depths), (e) fifth layer (18–21 m depths).
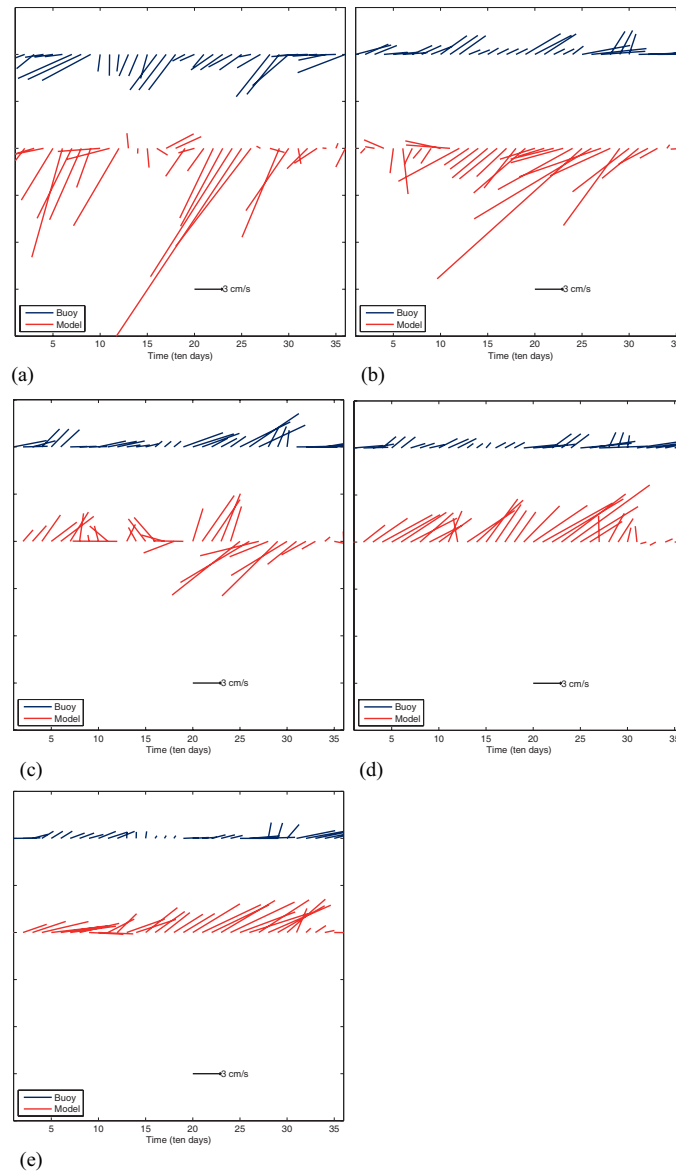
Fig. 9. – (a) Currents in the first layer (1–4 m depths)—Comparison of experimental and model data of the surface layer. Results are similar and a general pattern is showing that surface layer is dominantly driven by outflow current. (b) Currents in the second layer (5–8 m depths). Model results are showing strong outflow while observations are showing currents into the Gulf. (c) Currents in the third layer (9–13 m depths). In the first half of the year, results from model and observations are showing a similar pattern—inflow currents. However in the second half of the year the outflow is present in model while observations are showing inflow feature. (d) Currents in the fourth layer (14–17 m depths). In this layer results from model and observation are showing similarity through the whole year with significantly higher magnitude. (e) Currents in the fifth layer (18–21 m depths). Results from the buoy and model are similar and are showing predominantly inflow current. Moreover, values from the model are in all five cells showing higher values than those from the buoy.
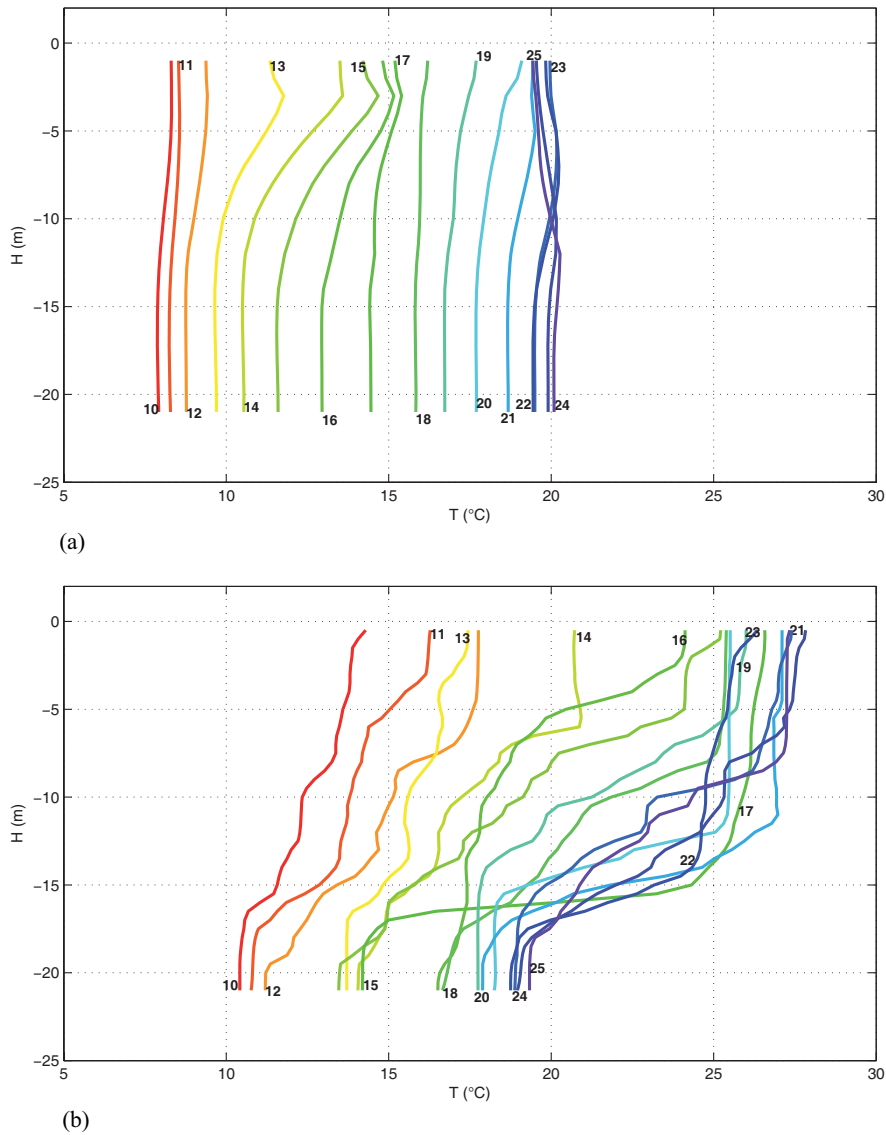
(a)

(b)

Fig. 10. – Vertical temperature profiles at COSP station, obtained from the model (a) within perpetual year and measurements (b) (numbers represent decade).

On the other hand, the vertical salinity profiles, which result from the model, are showing much stronger vertical gradients in the summer period (fig. 11a) than the measured ones (fig. 11b), with lower values of salinity than those measured between 2003-2006. It can be seen that the halocline in the model is deepening in the summer period and its lower edge reaches its maximum depth of around 18 m in the autumn period. Moreover, the climatic model also predicts a strong vertical difference of salinity between surface and bottom in the summer period ($\Delta S = 3$ PSU). This differs from the situation in the Gulf during summer where salinity values from the surface are similar to those near the bottom (fig. 11b).
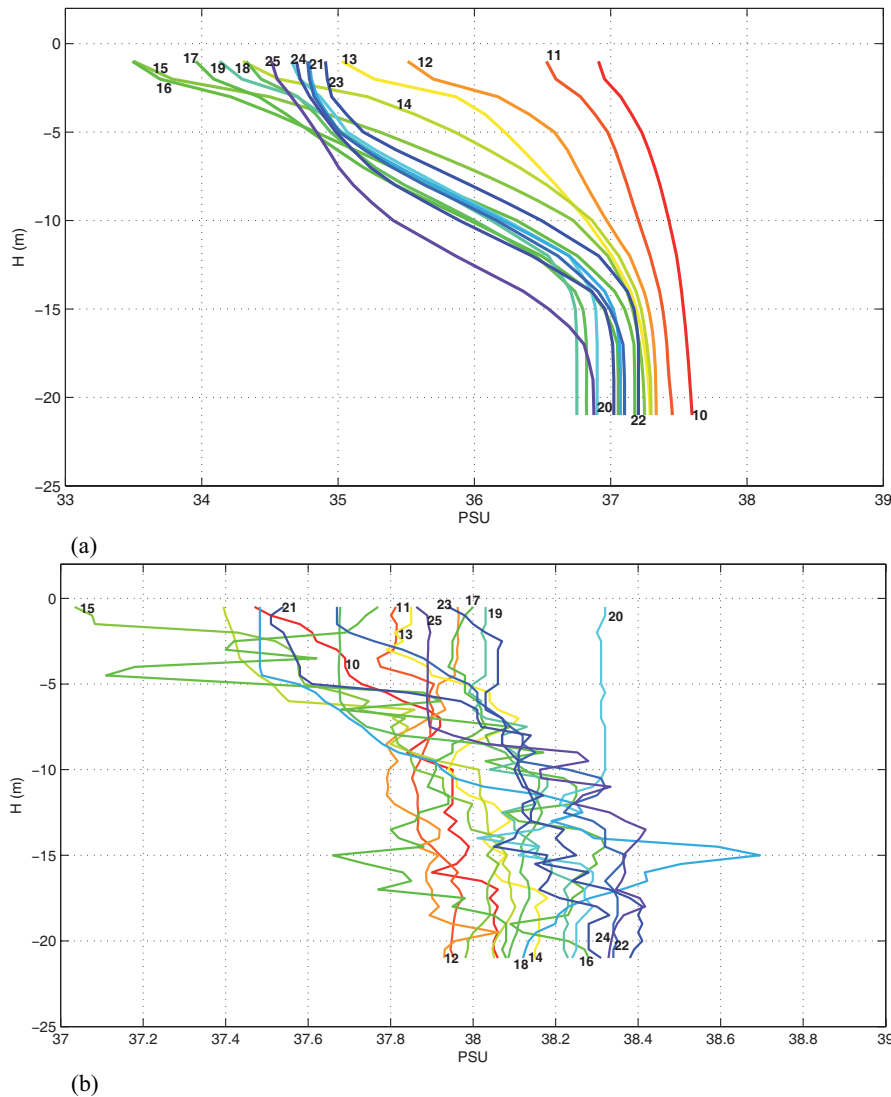
(a)

(b)

Fig. 11. – Vertical salinity profiles at COSP station, obtained from the model (a) within perpetual year and measurements (b) (numbers represent decade).

From salinity and temperature the vertical density distribution $\rho(T, S)$ was determined. It is clearly seen (fig. 12a) that the vertical distribution of density from the model is following that of salinity (fig. 11a). Moreover, the vertical density distribution from measurements (fig. 12b) shows stronger stratification in late spring and early summer (14-20 decades) at a depth of $5\,\mathrm{m}$ (1.5–$2\,\mathrm{kg/m^3}$) and at a depth of $15\,\mathrm{m}$ in autumn, while this is not the case with the model results. However, despite the lack of stronger stratification at the depths around $5\,\mathrm{m}$ and $15\,\mathrm{m}$ the model is otherwise showing a proper evolution of density stratification, where density values near the sea-bottom in the model in autumn are lower than the measured ones for about $1.3\,\mathrm{kg/m^3}$.
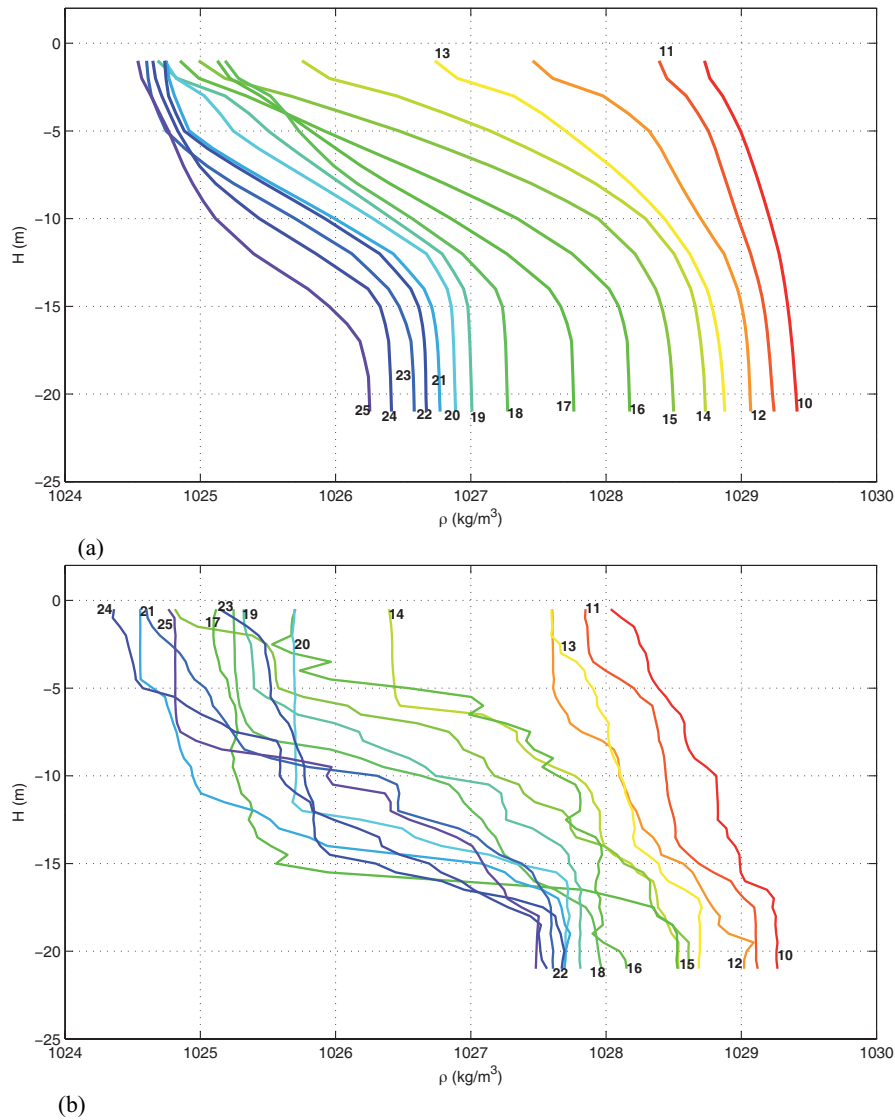
Fig. 12. – Vertical density profiles at COSP station, obtained from the model (a) within perpetual year and measurements (b) (numbers represent decade).

PCA was applied to model and experimental data of vertical stratification. The first three dominant PCA modes of modelled temperature at COSP show temperature variations along the vertical (fig. 13a upper) and in time (fig. 13a lower). The first mode represents 74% of the total variance while the other two dominant modes compose around 20% of the variance. Therefore, a reasonable understanding of the modelled stratification at COSP follows simply by looking at the first (barotropic) mode, since maximum values of the first mode of modelled temperatures are obtained in late summer and minimums in the late winter period. This evolution in time is roughly followed also
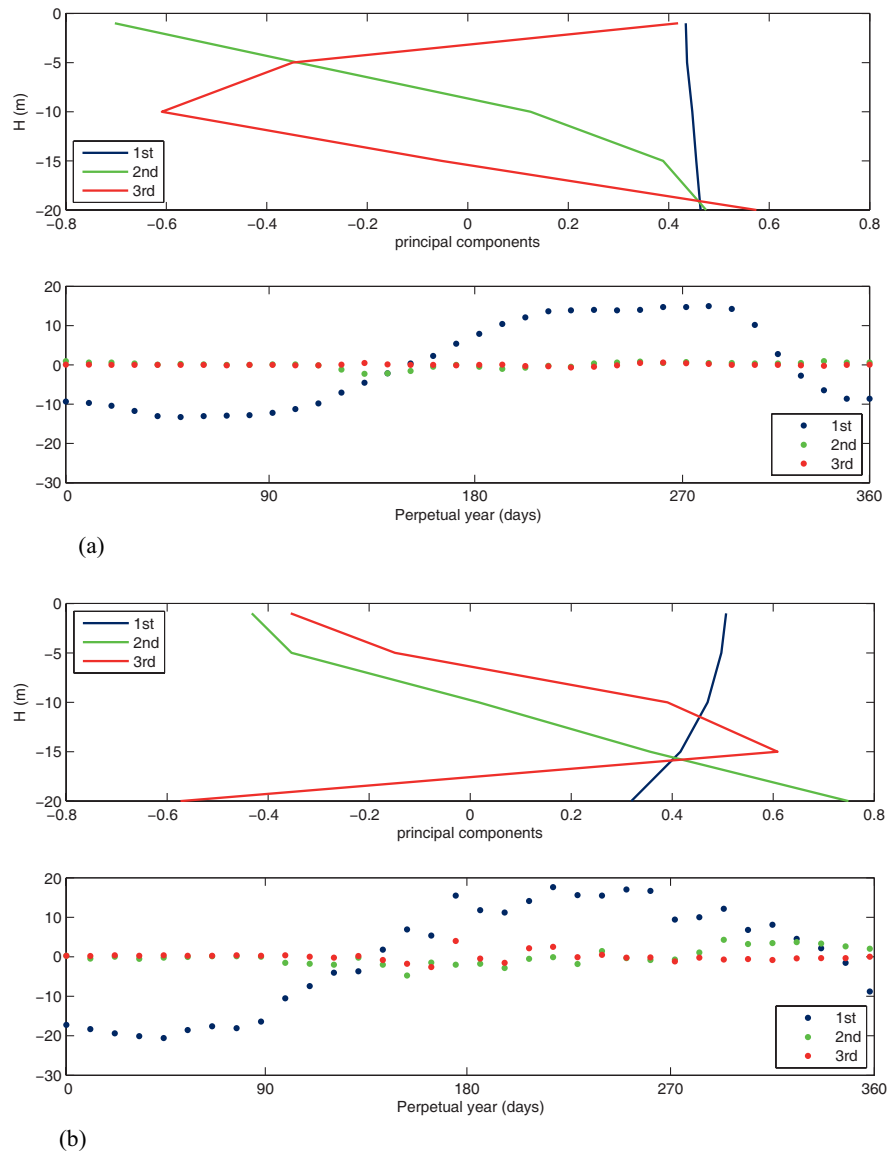
(a)

(b)

Fig. 13. – a) PCA of modelled temperature. Upper figure: the vertical distribution of temperature, first three modes that represent more than 90% of the variance of all data; 74% by the 1st mode, 17% by the 2nd mode and 4% by the 3rd mode. Lower figure: the variation of the modes during perpetual year. b) PCA of measured temperature. Upper figure: 74% by the 1st mode, 20% by the 2nd mode and 3% by the 3rd mode. Lower figure: the variation of the modes during perpetual year.

by the first mode of PCA on temperatures measured at COSP (fig. 13b, lower plot). The PCA modes of measured temperatures differ from the vertical distribution of the first three modes of modelled temperatures. The first mode is almost constant along the vertical (fig. 13a), while measurements show that the first mode is decreasing with depth (13b). The first mode of measured temperatures represents 75% of the total variance, while the second mode represents around 20% of the total variance. It follows from fig. 13b that the first mode of measured temperatures decreases with depth, while the first mode of modelled temperatures is slightly increasing with depth. The second mode of modelled temperatures is positive near the surface and bottom, while it is negative in the middle part of the water column. The second mode of measured temperatures is, on the contrary, positive in the middle part of the water column, and negative near the surface and bottom.

PCA of modelled salinities along the vertical at the location of COSP (fig. 14a) shows different vertical distribution of the first three modes than those of temperature. The first mode of modelled salinities represents 82%, while the other two modes represent only around 14% of the total variance. Salinity in the first mode is increasing with depth (fig. 14a top)—which is similar to the vertical distribution of the first mode of measured salinities (fig. 14b top). The second mode is positive at the surface and at the bottom, while it is negative at mid-depths with a minimum at the depth of 5 m. The first mode of modelled salinities is negative and is increasing with depth. It roughly varies seasonally, with a minimum in winter and two maxima, one in late spring and the other, larger one in late summer. However, the first mode of measured salinities is also negative, increases with depth and covers a much lower amount of the total variance (71%). The second one is positive at a depth of 5 m, negative at the surface and close to zero near the sea-bottom. The second and the third modes compose 22% of the total variance of measured salinities. The vertical profiles of measured salinities are also much more chaotic (fig. 11b), which resulted in a lower amount of the variance of the first mode. The vertical profile of the third mode of measured salinities (fig. 14b, top) roughly follows that of the modelled salinities (fig. 14a, top). Variations of modes over the year are much lower than those of the modelled salinities (fig. 14b, bottom).

The first two PCA modes of the vertical distribution of modelled density at the location of COSP are similar to the vertical distribution (fig. 15a, top) of modes of salinity. The first mode of modelled densities represents 79% of the total variance, while the other two modes compose 19%. The first mode of modelled densities is negative and increases with depth (fig. 15a, top), which is also a characteristic of the first mode of densities, calculated from the measured temperatures and salinities (fig. 15b, top). In the latter, however, the increase with depth is larger. The second mode of modelled densities is positive at the surface and near the bottom, while it is strongly negative in between, with the minimum at a depth of 5 m. At this depth the second mode of "measured" densities is near zero. It reaches a broader minimum at depths of 10–15 m, while it is positive near the bottom and at the surface. The third modes are actually opposed: while the one of modelled densities is decreasing with depth, the one of measured densities is increasing. Seasonal variation of the first mode of modelled densities is showing a minimum in winter and a maximum in autumn (fig. 15a, bottom). The first mode of "measured" densities (74% of total variance) roughly varies seasonally, with a broader minimum in winter and an especially wide period of maximal values in summer, which resembles the variations through a year of the first mode of the measured temperatures. The second and the third modes of the "measured" density compose 23% of the total variance.
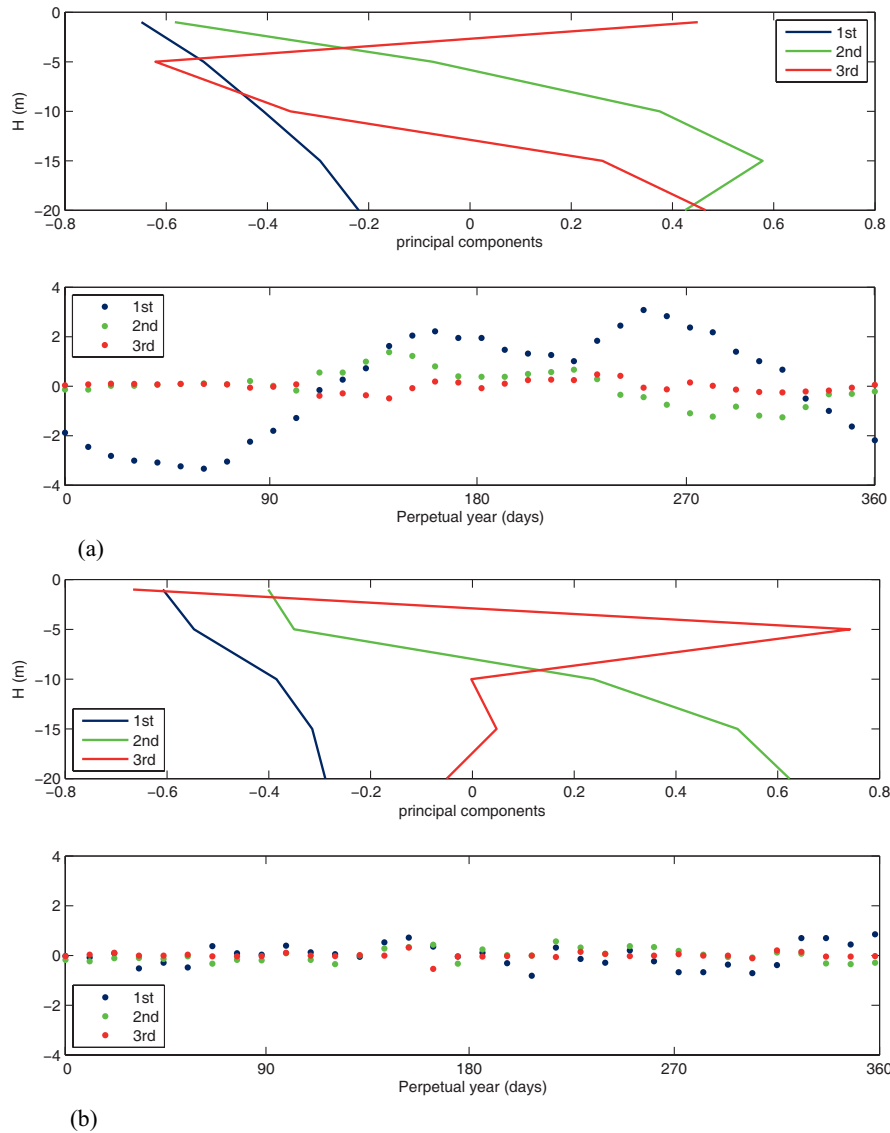
Fig. 14. – a) PCA of modelled salinity. Upper figure: the vertical distribution of salinity, first three modes that represent more than 95% of the variance of all data; 82% by the 1st mode, 14% by the 2nd mode and 3% by 3rd mode. Lower figure: the variation of the modes during perpetual year. b) PCA of measured salinity. Upper figure: 71% by the 1st mode, 17% by the 2nd mode and 5% by the 3rd mode. Lower figure: the variation of the modes during perpetual year.

3˙4. Wind stress and currents. – The monthly wind stress that is used as input for the model is having much higher values than the data measured at COSP (fig. 16 upper). It can be seen that wind stress from the model is significantly larger through all year by 20%–30%. This is particularly true for the autumn period, when differences between modelled and measured currents are the largest, but to a lesser extent also for the spring period.
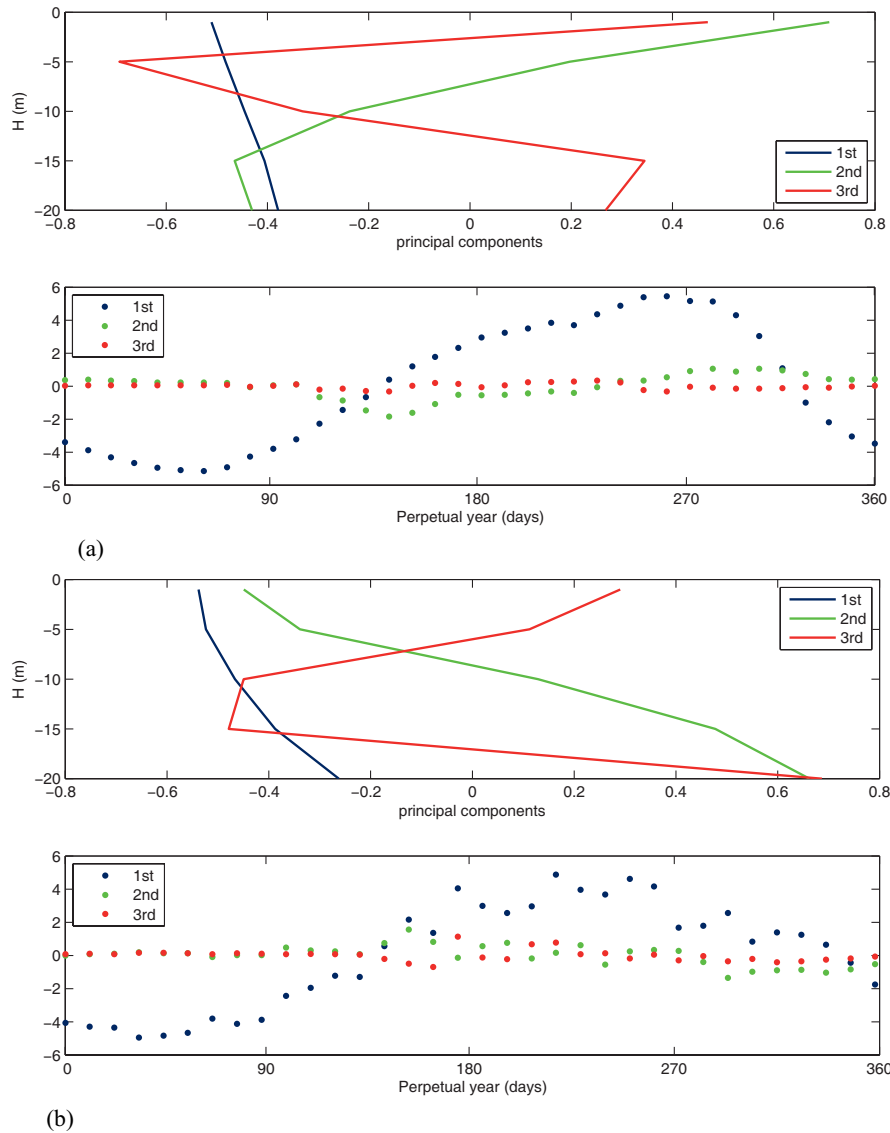
(a)

(b)

Fig. 15. – a) PCA of modelled density. Upper figure: the vertical distribution of density, first three modes that represent more than 90% of the variance of all data; 79% by the 1st mode, 15% by the 2nd mode and 4% by the 3rd mode. Lower figure: the variation of the modes during perpetual year. b) PCA of measured density. Upper figure: 74% by the 1st mode, 18% by the 2nd mode and 5% by the 3rd mode. Lower figure: the variation of the modes during perpetual year.

It was previously revealed that velocity magnitudes in model results are higher through all water columns than those measurements COSP. Differences in velocity magnitude between model and experimental data are decreasing with the water depth since the surface layer is most influenced by the bora wind. In the second and partially in the third layer velocity differs completely, in magnitude as well in direction, while in layers four and five in the bottom half of the water column the agreement between modelled and measured currents is much better, particularly in direction.
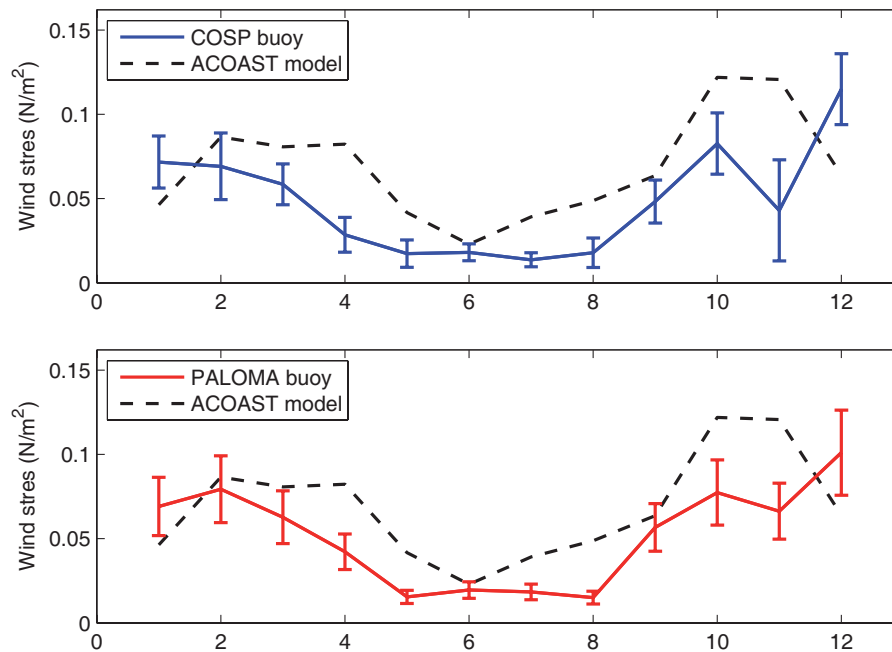
Fig. 16. – Wind stress. Comparison of experimental (COSP and PALOMA) and model results for wind stress in different times of the year. Values are quite unmatched particularly for winter and spring period where model results are showing higher wind stress and even some fluctuations. However, in summer period values are similar. The length of vertical bars denotes two standard deviations (minimum and maximum value of wind stress for a particular month).

The wind stress applied in the model was additionally validated with the wind data obtained from the PALOMA station for period 2006-2008, which is situated in the central part of the Gulf (fig. 1). Wind stresses at PALOMA and at the COSP stations are quite similar (fig. 16), while both of them are much smaller than the stress used in the model. Minor differences in wind stresses between the COSP and PALOMA stations are evident in February and November, when PALOMA has larger values and in October, when PALOMA has smaller values of wind stress than that at COSP.

4. – Conclusions

Since the Gulf is limited in size as well as in depth it is strongly influenced by weather conditions. The study of currents in the Gulf showed seasonal variations which is mainly related to the wind forcing (bora). This is particularly true for the surface layer of the water where mean currents are showing outflow in all seasons.

Inter-annual variability of mean currents is noticed in the surface layer during summer and autumn period. In summer period of 2003 and 2004 there were inflow currents while in autumn there were outflow currents at the surface. In years 2005 and 2006 a contrary situation appeared: in summer period outflow currents were present, while in autumn there were inflow currents.

In water layers that are below the surface layer (deeper than 5 m), interannual variability is not present and there are mainly inflow currents. They could be explained by

the dominant bora wind which is affecting only currents in the upper (surface) layer. The outflow in the surface layer piles up the water surface near Venice (fig. 1), which creates a counteracting pressure gradient force which drives the inflow in the Gulf in deeper layers.

In comparison between model and experimental results disagreement was noticed in magnitude for all layers and in directions for the middle layer. Through all water column model results produced much higher values of currents than those from the COSP. Disagreement in intensity of measured surface currents and modelled ones is related to the differences in the wind stress. Comparisons of the wind stress results calculated by methods [10] and [11] are showing very similar results. However, the approach by [12] yields significantly different wind stresses particularly for lower as well as higher wind velocities.

It is shown in this work that the climatic wind stress applied in the model is for up to 30% larger than the stress measured at COSP and PALOMA. This explains the major part of discrepancies in magnitude of currents between modelled values and measurements.

In future further adjustment of the wind stress in the model will be conducted where observations will serve as a reference.

The discrepancy in direction between the modelled and measured currents in mid-depths (5–13 m) is related to the stratification (vertical density gradients), particularly in the summer period. While modelled currents at this depth interval follow in direction the one near the surface (general outflow), the measured currents are already opposing the ones at the surface. This is related to the weaker vertical density gradient in the model at depths, especially around 5 m, which enables the penetration of surface momentum to larger depths. The model shows a strong reversal in the direction of currents between the layer of 9–13 m and the layer of 14–17 m. The separating depth is at 13.5 m, where again, the reproduction of a stronger vertical density gradient is missing in the model. This reversal in direction of currents should be reproduced at the depth of 4.5 m. Another peculiarity is related to stronger currents in the model in the bottom part of the water column (below 14 m). The generally stronger inflow at depths in the model is most probably related to the wind set-up and the general outflow at the surface—larger outflow from the Gulf needs to be compensated for by the larger inflow at depths.

Therefore, future studies will have to explore this discrepancy in the model. Agreement in direction of currents between model and measurements was found at the surface and in the two deepest water layers where the magnitudes of the modelled currents are closer to measurements than in the surface layer.

* * *

REFERENCES

[1] Crise A., Querin S. and Malačič V., *Acta Adriatica*, **47** (2006) 185.
[2] Dorman C. E., Carinel S., Cavaleri L., Sclavo M., Chiggiato J., Doyle J., Haack T., Pullen J., Grbec B., Vilibić I., Jeneković I., Lee C., Malačič V., Orlić M., Paschini E., Russo A. and Signell R. P., *J. Geophys. Res.*, **111** (2006) 3.

[3] MALAČIČ V., *Ecol. Model.*, **138** (2001) 173.

[4] MOSETTI F. and MOSETTI P., *Boll. Oceanol. Teor. Appl.*, **3** (1990) 251.

[5] MALAČIČ V. and PETELIN B., *Gulf of Trieste* in *Physical Oceanography of the Adriatic Sea, Past, Present and Future*, edited by CUSHMAN-ROISIN B., GAČIĆ M., POULAIN P.-M. and ARTEGANI A. (Kluwer Academic Press, Dordrecht) 2001, pp. 167-177.

[6] MALAČIČ V. and MARKOŠEK J., Technical report (Piran, Slo) 2006, p. 2.

[7] MALAČIČ V. and PETELIN B., *Acta Adriatica*, **47** (2006) 207.

[8] BEARDSLEY R. C. LIMEBURNER R. and ROSENFELD L. K., *Woods Hole Oceanographic Institution Technical report* (WHOI, USA) 1985, p. 234.

[9] EMERY W. J. and THOMSON R. E., *Data Analysis Methods in Physical Oceanography* (Elsevier, Amsterdam) 2001, p. 638.

[10] KONDO J., *Boundary Layer Meteorol.*, **9** (1975) 91.

[11] SMITH S. D., *J. Geophys. Res.*, **93** (1988) 15467.

[12] LARGE W., MORZEL J. and CRAWFORD G., *J. Phys. Oceanogr.*, **25** (1995) 2959.

[13] GIBSON J. K., KALLBERG P., UPPALA S., NOUMURA A., HERNANDEZ A. and SERRANO E., *ERA Description* (ECMWF, Reading, UK) 1997, p. 77.

[14] HELLERMANN S. and ROSENSTEIN M., *J. Phys. Oceanogr.*, **13** (1983) 1093.

[15] CAVALERI L. and BERTOTTI L., *Mon. Weather Rev.*, **125** (1997) 1964.

[16] ZVATARELLI M., PINARDI N., KOURAFALOU V. H. and MAGGIORE A., *J. Geophys. Res.*, **107** (2002) 20.

[17] ZVATARELLI M. and PINARDI N., *Ann. Geophys.*, **21** (2003) 345.

[18] ARTEGANI A., BERGANT D., PASCHINI E., PINARDI N., RAICICH F. and RUSSO J., *J. Phys. Oceanogr.*, **27** (1997) 1492.

[19] KILLWORTH P. D., *J. Phys. Oceanogr.*, **26** (1996) 136.

[20] MARSALEIX P., ESTOURNEL C., KONDRACHOFF V. and VEHIL R., *J. Mar. Syst.*, **14** (1998) 99.

[21] RAICICH F., *J. Mar. Syst.*, **9** (1996) 305.

[22] MALAČIČ V., CELIO M., ČERMELJ B., BUSANI A. and COMICI C., *J. Geophys. Res.*, **111** (2006) 3267.